ECOHYDROLOGICAL ANALYSIS IN A FOREST ECOSYSTEM OF SEASONAL VARIATIONS IN THE MOISTURE CONTENT OF CLAY-RICH SOIL

A Thesis

by

KATHIE ALEXANDRA GUERRA

Submitted to the Office of Graduate and Professional Studies of
Texas A&M University
in partial fulfillment of the requirements for the degree of

MASTER OF SCIENCE

Chair of Committee,	Mark Everett
Committee Members,	Peter Knappett
	Georgianne Moore
Head of Department,	Julie Newman

May 2020

Major Subject: Geophysics

ABSTRACT

Soil water availability influences the physiological, structural, and functional properties of plants. The physical properties of the soil play an important role in determining water availability, and shapes both the root distribution and tree adaptability to changes in weather and climate. Electrical resistivity tomography (ERT) is a nondestructive geophysical method that images spatiotemporal variations in bulk soil resistivity, which, in turn, can be related to variations in soil water content. The goal of acquiring ERT data is to help ecohydrologists to better understand how seasonal variations, climate change and land usage can affect hydrologic fluxes and the sustainability of an ecosystem. My study analyzes the soil moisture regime in Danciger, a forested site located in the San Bernard watershed floodplain in Brazoria County, Texas. Additional data from nearby Dance Bayou and Otto forested sites were also obtained. These soils are composed primarily of clay. Clays increase the overall bulk electrical conductivity of a soil due to their negative surface charges that create an efficient electrical conduction pathway. An important objective of my study is to understand how soil moisture content and water uptake from the trees affects the ERT response. The goal is to better understand the soil-water dynamics in relation to the water needs of the plants. To observe subsurface soil moisture variation caused by seasonal weather variations, several ERT surveys were collected throughout the year. The resulting time-lapse geophysical images provide spatiotemporal information about the ecohydrological processes of the trees that pertain to soil moisture variations within the root zone. The results suggest that tree water uptake depletes soil water content in the root zone during the growing season.

Surficial soil moisture could be redistributed by the roots, decreasing the soil moisture in deeper zones. Deep soil moisture remains relatively unchanged throughout the year, possibly indicating that water infiltration is low in the clay-rich soil for most of the year. Some infiltration was inferred after the winter. The ERT results are compared to laboratory experiments that correlated resistivity to soil moisture in order to constrain the geophysically-determined estimates of the water content in the soil.

DEDICATION

I dedicate this thesis to my parents Oscar Guerra and Katty Aciego for their unconditional care, love, and support. This work and my previous accomplishments would not have been possible without them.

I also dedicate this thesis to Oscar Dominguez for offering me his love and support throughout these years.

ACKNOWLEDGEMENTS

I would like to thank my committee chair Dr. Mark Everett and my committee members Dr. Peter Knappett and Dr. Georgianne Moore for their support, guidance, and mentorship throughout the course of this project.

I would also like to thank those who traveled with me to the research sites and lent me their hands during the ERT data collection process: Mark Everett, Ajinkya Deshpande, Austin Zen, Deanroy Mbabazi, Ashley Cross, and Aaron Trimble.

Special thanks go to the researchers in the ESSM and BAEN departments at Texas A&M for sharing the data they collected for their studies, and the TWO for providing additional data.

Special thanks go to my friends and family that supported and encouraged me throughout the whole journey, making my time at A&M an amazing experience.

Lastly, I would like to mention the scholarships, fellowships and grants that allowed me to complete my studies at Texas A&M University: Roland & Margaret Prove Student Scholarship, Association of Former Students Scholarship, Crocker, George W. Scholarship II, Good Neighbor Scholarship, Lechner Scholarship, Halbouty ’30 TAMU AAPG Fellowship, and Texas Public Education Grant.

CONTRIBUTORS AND FUNDING SOURCES

Contributors

This work was supervised by a thesis committee consisting of Professor Mark Everett and Professor Peter Knappett of the Department of Geology and Geophysics and Professor Georgianne Moore of the Department of Ecosystem Science and Management.

The data analyzed was collected and processed using the instrumentation and software provided by Professor Mark Everett. The data was collected primarily by myself, with the aid of Professor Mark Everett, Ajinkya Deshpande, Ashley Cross, Austin Zen, and Aaron Trimble from the Department of Ecosystem Science and Management and Deanroy Mbabazi from the Department of Biological and Agricultural Engineering.

Additional data was provided by the Texas Water Observatory researchers Ajinkya Deshpande and Ashley Cross from the Department of Ecosystem Science and Management, and Amir Sedaghatdoost and Deanroy Mbabazi from the Department of Biological and Agricultural Engineering.

All other work conducted for the thesis was completed by myself independently.

Funding Sources

There are no outside funding contributions to acknowledge related to the research and compilation of this document.

TABLE OF CONTENTS

Page

LIST OF FIGURES

Page

LIST OF TABLES

Page

1. INTRODUCTION

Plants require different amounts of water and different levels of soil moisture to sustain themselves and grow (Jayawickreme et al., 2008). Their needs vary seasonally within a single ecosystem (Bass et al., 2017). As weather changes, so do the physiological functions and structures of plants (Vasellati et al., 2001; Stratópoulos et al., 2019). Their interactions with the subsurface alter the soil moisture dynamics and controls their ability to extract water and nutrients from the soil (Rodríguez-Robles et al., 2017). The water availability determines the capacity of a plant to carry out its basic life functions, such as photosynthesis, transpiration, respiration, and decomposition of organic matter. Furthermore, soil moisture impacts other aspects of ecohydrology, such as microbial composition in the soil and groundwater discharge into rivers, streams, and wetlands (Rodríguez-Iturbe et al., 2007). In more general terms, as stated by Jayawickreme et al. (2008) "*characterizing the dynamic interactions between vegetation and soil moisture is critical to forecast global water resources and improve land-atmosphere feedback models*."

1.1. Plant Physiology and Water Movement

Plants depend on recent rainfall and the soil moisture it induces as the main source of water (Dobson, 1995). Forests with large closed canopies intercept a substantial amount of the precipitation since the leaves, branches, and trunks comprise a relatively impermeable barrier (Shang, 2016). The intercepted water may be evaporated, absorbed by the leaves, dripped onto the ground (throughfall), or it may run down the stems of the trees to the ground (stem flow) (Chapin III et al., 2002). Typically, 10-50% of intercepted

water does not reach the soil. Most of the water that reaches the soil from the canopy comes via throughfall. Thus, the canopy surface area (mainly leaves) and its spatial heterogeneity greatly influence soil moisture spatial variability. The heterogeneity of the canopy determines its capacity to intercept and store water. (Chapin III et al., 2002)

Once the water reaches the soil, it can infiltrate into subsurface pore spaces depending on the type of soil and its compaction. Soil consist of a grain matrix and pore space, the latter being filled with air and water (Amidu and Dunbar, 2007). The pore space, which contain water and air, is the major water reservoir in most ecosystems. The volumetric water content of the soil is the ratio of the volume of the water to the total volume of the soil, including the pore space and the grains (Fetter, 2001). Once the storage capacity in the pore spaces is exceeded, water will drain into groundwater aquifers or escape to the surface as runoff. Soil water can also be depleted through evaporation and transpiration by plants (Jackson et al., 2000; Bass et al., 2017). Fine-textured, deeper soils typically have more pore space volume than rocky/sandy, shallow soils. For this reason, clay soils retain more water than sandy soils. Uncompacted soils also hold more water than compacted soils. The general rule is that “water is held more effectively by small soil pores that have a large surface-to-volume ratio” (Chapin III et al., 2002; Jackson et al., 2000).

The infiltration capability of soil depends on the hydraulic conductivity and preferential flow of water through macropores (Chapin III et al., 2002). Hydraulic conductivity refers to the ease by which water flows within the pore space, and it depends on the intrinsic permeability of the soil, the grain size of the sediment, and the density and

viscosity of the fluid (Fetter, 2001). Hydraulic conductivity is lower for partially saturated porous media. Saturation is defined as the ratio between the volume of the water and the volume of the pore space (Fetter, 2001). Relative to air, water is the wetting-phase on the surface of minerals. When enough pore spaces are saturated, a network of connected pore spaces allows water to be transmitted.

Hydraulic conductivity is limited primarily by the grain size of the sediment. Fine clay soils have very low hydraulic conductivity, which prevent water percolation into deeper soils. Even though clay soils have higher porosity, coarser sandy soils with low porosity allow water to more readily infiltrate (Fan et al., 2017). Aquifers underlying clay soils tend to have shallow water tables for this reason. Gravitational forces pull water downward, but some water remains adsorbed to the soil particles and retained within pore spaces. Additionally, hydraulic conductivity of a given porous media declines significantly in dry soils since water can flow around air-filled pores, thereby taking a longer, tortuous path. Flow-path tortuosity makes it difficult for plants to obtain water. Thus, the hydraulic conductivity of the soil limits the rate of replenishment of soil water to a larger extent than the hydraulic conductivity of the plant itself (Jackson et al., 2000; Rothfuss and Javaux, 2017; Shang, 2016). In clay loam and clay, the volumetric water content in the soil must be in the range 10-40% to be available for plants (Fetter, 2001).

The driving force for root water uptake is the water potential difference in transpiring plants, moderated by stomatal conductance and atmospheric demand (Rothfuss and Javaux, 2017; Jackson et al., 2000). The absorbed water flows through the roots to the leaves through pathways of transport tissue called xylem vessels. Water flows upward

against gravity due to the positive hydraulic potential difference that exists between the leaves and the ground. Most water absorbed by tree roots is lost to the atmosphere through evapotranspiration that takes place in the leaves (Jackson et al., 2000; Rothfuss and Javaux, 2017). As leaves absorb CO_2 for photosynthesis through their stomata, they also release water into the atmosphere. Transpiration is strongly related to soil moisture content and hydraulic conductivity; dryer soils inhibit water transfer into the leaves and could lead to stomatal closure (Shang, 2016). Temperature can also influence transpiration.

1.2. Root Water Uptake

Root water uptake depends on the spatial distribution of the roots in the soil. The latter is affected by the soil water profile and the groundwater drainage, and the hydraulic properties of the roots (Fan et al., 2017; Rothfuss and Javaux, 2017). According to Crow (2005), root distribution is determined by the soil properties, tree species, age and health of the tree, and various other environmental factors. Root distribution is often very shallow, usually < 2 m in depth, with 90% of the roots in the upper 60 cm (Crow, 2005; Dobson, 1995; Chapin III et al., 2002). In the uppermost layers, the soil is loosely consolidated and nutrients, water and oxygen are readily available. Clay soils readily retain moisture, so trees growing over clay soils do not grow deep roots compared to trees growing on loosely consolidated, dryer soils (Crow, 2005). Fan et al. (2017) correlated root depth to water table depth and found that shallow water tables can cause roots to accumulate at shallow depths, while deeper water tables cause roots to grow downward. During dry periods, roots tap soil moisture from deeper soil horizons (Jipp et al., 1998; Bass et al., 2017). An electrical resistivity study performed by Bass et al. (2017) showed

that shrubs and junipers in semi-arid climates were able to access water from both shallow and deeper soil horizons during droughts. This observation suggests a hydraulic redistribution as the roots capture water. After a rainfall event, the authors observed that water intake returned to the shallow soil horizons via hydraulic redistribution. In those zones, water flows preferentially through macropores and root channels.

Roots have a higher hydraulic conductivity than soils, so water flow mores easily through the roots. When water enters the roots, the adjacent soil particles lose water and the thickness of the water film around the particles decreases. This creates a local water potential reduction near the roots that draws in moisture from higher-potential zones (Chapin III et al., 2002). Roots grow fine roots and root hairs to increase the surface area in contact with the soil (Vasellati et al., 2001, Crow, 2005). The contact area is reduced however as the soils dry and shrink, especially in clay soils, since the air content of the pore spaces increases.

Plants adjust their physiological, structural and morphological functions according to seasonal variations in soil moisture content, i.e. during wet and dry periods (Vasellati et al., 2001; Stratópoulos et al., 2019). Root xylem are more prone to cavitation, or filling with air, than stem xylem (Jackson et al., 2000), especially the xylem vessels with large diameters. Cavitation in the root xylem can obstruct water flow. For this reason, the xylem diameter in some plants decreases during droughts. This increases the tension of the water column inside the xylem and hence the resistance to water flow. Since less water is absorbed, dry seasons reduce the growth and development of plants (Vasellati et al., 2001; Jackson et al., 2000). Plants also store internal water, reduce the leaf surface area, and

extend their root systems to avoid extremely negative water potentials (Stratópoulos et al., 2019). Typically, in dry climates, the plant water potential balances the soil water potential, so water can flow from deeper soils into the roots. This process is known as hydraulic lift (Jackson et al., 2000; Chapin III et al., 2000).

During wet periods, the excess of water does not allow the roots to retrieve oxygen from the pore spaces between the soil particles. This is because the saturating water causes waterlogging, creating hypoxia that leads to anoxic conditions (Parent et al., 2008). Respiration declines during wet periods and reduces stomatal conductance and water uptake. Furthermore, plants growing in flood-prone areas tend to have a decreased number of root hairs and an increased number of aerenchyma, which are soft plant tissue containing air spaces (Vasellati et al. 2001), to compensate for the lack of oxygen in the soil. It is important to understand the relationships between trees, precipitation, weather changes, and water availability because of long-term effects of global climate change, especially for forested areas that may not be immediately adaptive to rapid changes in climate.

1.3. Electrical Resistivity Tomography (ERT)

Geophysical techniques that probe near-surface water content can assist ecohydrologists to determine the groundwater-vegetation dynamics of ecosystem. Currently, a main limitation to such determinations is the inability to accurately characterize transient water fluxes (Bass et al., 2017; Jayawickreme et al., 2008). A common geophysical technique, electrical resistivity tomography (ERT), allows geophysicists to image the subsurface based on the resistivity (or its reciprocal,

conductivity) of the ground at shallow depths up to 20 m (Bass et al., 2017). Electrical conductivity is defined as the ability of a material to sustain a long-term electric current flow, in this case by means of the migrating ionic charge carriers comprising the pore-fluid electrolyte (Everett, 2013). Time-lapse ERT images can be used to calculate transient water fluxes since varying degrees of soil water content elevates the bulk surface conductivity. Specifically, bulk electrical resistivity is sensitive to soil water content, bulk density, and, especially in clays, surface conductivity of the soil particles (Laloy et al., 2011).

ERT is a nondestructive geophysical method that can be used to monitor spatiotemporal variations in bulk soil conductivity, which in turn are related to soil water dynamics (Amidu and Dunbar, 2007; Rodríguez-Robles et al., 2017). The technique involves injecting a current into the ground across one pair of electrodes of a linear array, reading the resulting voltage across another pair of the array, and then converting a pre-arranged set of such readings into a map of electrical resistivity of the soil. The impressed voltage across the two current electrodes causes mobile charges, principally ions, in the subsurface to migrate according to their mobility. Charge carriers that are bound to an atom lattice cannot migrate and hence they do not affect ERT measurements. The resulting voltage distribution caused by the subsurface current flow is measured along the array across pairs of electrodes acting as voltmeters. The measured voltages are transformed into apparent resistivity measurements, as described below. Then, the latter are converted into a 2D Earth resistivity image by a tomographic inversion. The image is that of soil bulk resistivity plotted as distance along the electrode profile vs. depth below the surface.

Reducing the spacing between electrodes yields an image at higher spatial resolution, although the depth of penetration is decreased. Generally, the depth of penetration is ~1/3 of the electrode array length.

Geophysicists assume that the Earth has a uniform resistivity for deriving an apparent resistivity from a measured voltage value. Variations from a homogeneous Earth are caused by anomalies. They account for the actual heterogeneity within the Earth's subsurface. The term *apparent resistivity* ρ_a is the ratio between the measured voltage and the injected current multiplied by a geometric array factor *k*. The geometric factor depends on the spacing between electrodes and the type of electrode array used (Dictionary of Earth Sciences, 1999). Apparent resistivity has the same units [Ωm] as resistivity and is interpreted as the resistivity that the Earth would have, based on the measurements made, if it actually was homogeneous.

1.4. Electrical Measurements and Soil Moisture Content

Soil type affects the performance of ERT geophysical methods. In particular, the spatial distribution of salinity and saturation of the pore-fluid electrolytes affects the bulk electrical conductivity of the subsurface. Most soils conduct electric current via migration of the constituent ions in the pore fluid; this is the familiar process known as electrolytic conduction. Different soil types have different ranges of bulk conductivity. Clay has a particularly wide range, making its moisture content challenging to analyze by the ERT method. The bulk conductivity of clay soils depends on multiple physical factors, as discussed below. Geophysicists must consider additional pedological variables when working in clay environments than in silty or sandy soils.

The bulk conductivity of a soil medium is also affected by porosity. Porous fine-grained soils fully or partially saturated with electrolytes sustain electric current more easily than coarse-grained dry soils. Clay is more conductive than sand because of its higher proportion of pore space; also, the surfaces of platy clay minerals contain mobile electric charges. Similarly, pore-fluid salinity increases conductivity in clays since dissolved ions increase ionic exchange and promote the transfer of a current. Soils at higher temperature exhibit increased mobility of the constituent ions and hence are generally more conductive than soils at lower temperatures. According to Laloy et al. (2011), bulk soil conductivity can be related to soil moisture content by using a petrophysical relationship, or "pedo-electrical function", to represent soil conductivity. The soil type influences the form of the pedo-electrical function used by hydrogeologists and soil scientists.

Sandstones are typical porous media characterized by a well-interconnected pore space. If also well-sorted, sandstones can be very permeable to the flow of groundwater. Archie's Law (1942) describes the bulk electrical conductivity of a partially saturated, ideally clay-free, sandstone:

$$\sigma = a\sigma_W S_W^n \varphi^m \quad (1)$$

The variables in the above equation are:

σ = bulk conductivity;

a = leading coefficient, which varies widely dependent on pore cementation, grain size and shape, wettability, clay content, tortuosity, and other factors;

n = saturation exponent empirically determined to be ~2.0;

m = cementation exponent, dependent on grain shape, texture and cementation, and can range from 1.2-2.3 for sandstone;

σ_W = electrical conductivity of pore electrolytes depending on salinity, can range from 0.3-1.0 S/m;

S_W = level of saturation between 0 (dry) and 1 (fully saturated); ratio between volumetric water content and porosity

φ = porosity

Commonly, fully saturated sands at S_W = 1 are characterized by an intrinsic formation factor *F*, which is defined as the ratio between the electrical conductivity of the pore electrolyte σ_W and the bulk conductivity σ

$$F = \frac{\sigma_W}{\sigma} \tag{2}$$

The formation factor typically obeys $F > 1$ since the conductivity of the pore fluids exceeds the bulk value, except in some clays. According to many authors, the intrinsic formation factor is related to porosity by $F \sim \varphi^{-m}$

Archie's equation (1) was developed for clean sandstones and it assumes that electric current is conducted almost entirely through the pore fluid (Amidu and Dunbar, 2007). The formula for the bulk conductivity of a sandstone becomes more complicated in the presence of clay. Clay minerals that originate from secondary diagenetic processes are much finer than sand particles. Thus, clay particles tend to clog the pore space between sand grains. This clogging can result in reduced porosity and permeability, causing potentially high variability in the Archie parameters (*a, m*). Clays also increase the overall bulk electrical conductivity values due to the negative surface charges that create alternate

electrical conduction pathways (Everett, 2013). Archie's equation does not predict accurate bulk conductivity if used for soils with a high clay-content. A modification to equation (1) is required to account for the presence of clay.

Waxman and Smits (1968) developed a modified version of the intrinsic formation factor and called it the apparent formation factor F_a,

$$F_a = F\left[1 + \frac{\tilde{\sigma}}{\sigma}\right]^{-1} = \frac{\sigma_W}{\sigma + \tilde{\sigma}} \tag{3}$$

The term $\tilde{\sigma}$ in equation (3) accounts for the excess conductivity due to the cation exchange associated with the surface conduction in clay particles (Ali Swaid, 2009). The value of $\tilde{\sigma}$ depends on the clay mineralogy and concentration of the saturating electrolyte, but can be obtained from common electrochemical tables. The Waxman-Smits model (3) assumes that two parallel resistances develop from the pore fluid and the clay layers. Two limitations of this model are the assumptions that the surface conduction on clay particles is constant (Laloy et al., 2011) and that the electrolyte exchange cations are evenly distributed instead of being localized to the surfaces of the clay particles (Ali Swaid, 2009).

Doussan and Ruy (2009) performed a study of the electrical conductivity of three different types of soil: loam, silty clay loam, and sand. They measured the variations in electrical conductivity with water saturation and compared their results to the predicted values of the Waxman-Smits model. They determined that the Waxman-Smits model fit their results for sand and loam, but not for silty clay loam. At saturations less than 56%, Waxman-Smits underestimates the bulk electrical conductivity, as shown in Figure 1.

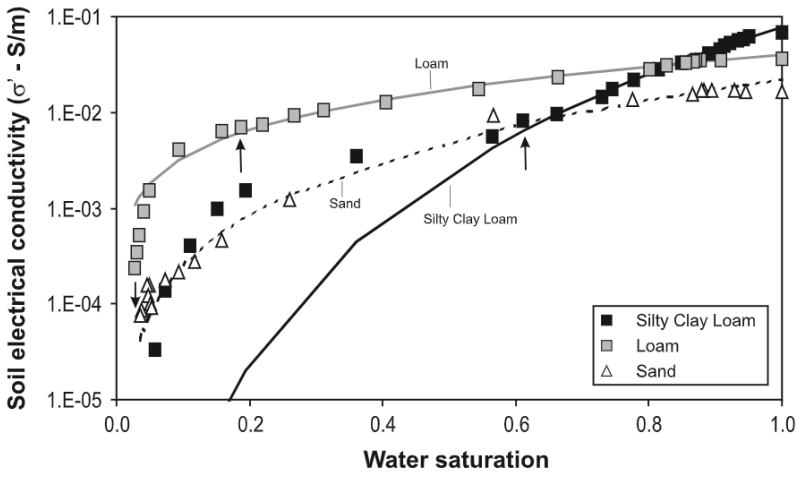

Figure 1. Bulk electrical conductivity as a function of water saturation for three types of soil: silty clay loam, loam, and sand. The symbols represent measured data and the curves represent the predicted trend based on the Waxman-Smits model. Reprinted with permission from 'Prediction of unsaturated soil hydraulic conductivity with electrical conductivity by C. Doussan and S. Ruy, 2009. *Water Resources Research,* 45, W10408, Copyright 2009 by John Wiley and Sons.

Other bulk-conductivity models for water saturation are available that are similar to the Waxman-Smits model by accounting for clay conductivity. For example, the Revil et al. (1998) model recognizes that surface conduction is independent of pore fluid salinity in clay-rich soils (Laloy et al., 2011). The Schlumberger dual-water model separates the bound water in clay from the bulk water, assuming that the exchange cations only contribute to the conductivity of the clay-bound water. This model can be used for dispersed or structural clay models. The dual water model predicts lower water saturation values than most other models. This prevents the geophysicist from incorrectly attributing low-resistivity measurements to higher water content in conductive clay soils (Onovughe and Sofolabo, 2016).

Swaid (2009) discusses the Clavier and Bussian models, which are similar to the Waxman-Smits model. Bussian's model accounts for different conduction pathways, thus it is useful for heterogenous mixtures that have distinctive components with different conductive properties. Clavier's model takes into consideration both free water and clay-bound water found between the clay electric double layer. Clavier assumes that the two fluids have different conductive properties, unlike the Waxman-Smits model. Nevertheless, Clavier's model requires knowledge of the amount of clay-bound water found in the double layer and a distinction is made between the clay-bound water and the pore-space free water (Ali Swaid, 2009).

To properly use these models, however, certain parameters must be determined that are specific to the type of soil being analyzed. All authors empirically determined the parameters through laboratory experiments and soil core analysis. An accurate soil moisture conversion would however require a knowledge of the horizontal and vertical spatial distribution and petrophysical parameters of the clay content. Assuming a single value for these parameters, valid at all locations, would not yield accurate results for a heterogenous medium. Such a complex soil analysis, is beyond the scope of this study. Instead, I compare my resistivity results to empirical relationships from the literature using similar soils as the ones found in my study area.

The resistivity tomograms obtained during the study are converted into a map of soil-moisture content using either the Waxman-Smits relationship (equation 4, below) or empirical laboratory-based relationships from the literature.

$$S_W = \left(\frac{\sigma - \tilde{\sigma}}{a\sigma_W \varphi^m}\right)^{-n} \quad (4)$$

The ERT-derived subsurface distribution of soil moisture reveals areas of low and high water-content. At my study site, the electrical conductivity of the pore electrolyte σ_W can be obtained from direct measurements with a handheld conductivity probe of standing water in a nearby slough. The bulk soil conductivity σ is obtained from the ERT resistivity tomogram. The porosity φ is obtained from a soil analysis, but to estimate the excess conductivity $\tilde{\sigma}$ due to clay fraction requires additional laboratory measurements of soil samples obtained from different depths across the ERT profile. Onovughe and Sofolabo (2016) describe three methods for soil analysis, but there is considerable uncertainty due to the limited resolution of resistivity logs and the inaccuracy of laboratory measurements and clay content assessments. Thus, obtaining an accurate $\tilde{\sigma}$ value is difficult and beyond the scope of this study.

Several studies have used ERT to analyze seasonal changes in soil moisture content (Amidu and Dunbar, 2007; Cardenas and Kanarek, 2014). Jayawickreme et al. (2008), Bass et al. (2017), and Rodríguez-Robles et al. (2017) used similar methods to correlate moisture variations to vegetation differences, root-water uptake, and weather variability to better understand the ecohydrological processes in their respective areas. Jayawichreme et al. (2008) studied time-lapse ERT of a cold, temperate forest and grasslands overlying predominantly fine sands. They collected ERT images from October 2006 to September 2007, spanning a full seasonal cycle. They followed the assumption that resistivity decreases with increasing water content. Their results show that resistivity was higher during the growing season when evapotranspiration is higher and decreased after sustained rainfall. The images also show that the differences in rooting depth between

the forest and the grassland also affect resistivity. The infiltrated water below the grassland drained deeper than the water below the forest. During dry periods, the resistivity increased within the upper 2 m, suggesting preferential water uptake of soil moisture near the surface. Additionally, the soil moisture deficit extended deeper below the forest than below the grassland. This study illustrated how seasonal variations in precipitation across two different ecotones can have contrasting effects on soil moisture distribution due to differences in root depth and water demands.

Bass et al. (2017) also used time-lapse ERT to study a semiarid hillslope with grasses, creosote bushes and junipers during a drought period with varying carbonates, silts and clays. The vegetation in this semiarid region can consume water from both shallow and deeper water horizons. Bass et al. obtained ERT images for four different transects covering a full seasonal cycle from November 2010 to August 2011. Their results showed higher resistivity depths during the drier summer season. As the drought progressed, the deeper resistivity increased as the water demand increased. Some shallower areas showed a decrease in resistivity, suggesting hydraulic redistribution. After the onset of monsoonal storms, the resistivity decreased in the shallow soils. Their ERT results coincided with the expected root water uptake capture zones for junipers and creosotes. The study suggests that the ERT method can accurately characterize temporal soil moisture changes in the subsurface.

Rodríguez-Robles et al. (2017) performed an 8-month ERT study in a semiarid pine-oak forest ecosystem overlying an impermeable, fractured rhyolitic bedrock. These soils have very low water storage capacity. They used ground-penetrating radar (GPR)

and ERT to study the root and water distribution. The subsurface root diameters and depths were estimated using the GPR method. The ERT images showed a detachment of the rock layers and soil pockets from weathered bedrock that can increase water storage and favor the anchorage of trees in limiting conditions. Combining both geophysical methods provided the authors with insight on pine and oak root water uptake patterns in the area that allow both tree species to coexist; pines absorb water from shallow horizons whereas oaks can access water in deeper weathered bedrock. Thus, ERT can be useful to understand seasonal ecological interactions in unfavorable weather conditions.

The objective of my study is to use a similar time-lapse ERT analysis of soil moisture variations in correlation to the ecohydrological processes, uniquely focusing on clay-rich soils underlying bottomland hardwood forests in humid subtropical climates. Areas near the Texas coast are particularly vulnerable to thunderstorms, hurricanes and flooding. The ERT results can provide insight on the effects these weather patterns have on water availability for vegetation overlying clay-rich soil. I will compare my results to empirical relationships from the literature to estimate the soil moisture across the study area.

2. METHODS

ERT measurements are acquired in the field by laying out a linear array of, commonly, 56 electrodes at a certain spacing, such as 0.5 m as for my study. Other numbers of electrodes and their spacing can be selected according to the survey objectives at hand, depending on the desired resolution and depth of penetration. For this study, a command file was programmed in the Advanced Geosciences Inc. SuperSting (AGIUSA, 2017) instrument console specifying a dipole-dipole configuration, in which the current and potential electrode pairs are separated by a pre-determined sequence of spacings up to 10 m. This configuration produces a response that can probe to a depth of ~6.5 m based on the 27.5 m array length. This depth of penetration is sufficient to image water uptake activity from the tree roots (Crow, 2005). Besides dipole-dipole, there are two other commonly used electrode configurations: Schlumberger and Wenner arrays (Everett, 2013). The Schlumberger array is ideal for deeper surveys and provides good vertical resolution as it creates a “virtual borehole”, while the Wenner array provides good lateral resolution as it creates a “virtual trench”. The dipole-dipole configuration used in this study combines the advantages of Schlumberger and Wenner. The dipole-dipole pseudo-section is interpreted after its conversion to a tomographic image, as described above. The instrument used supports simultaneous measurements recorded on multiple source-receiver channels, thus reducing the survey time. For my purposes, the dipole-dipole is an ideal configuration since I am interested in the lateral variations of soil water dynamics that occurs within the root-zone of the trees (about 2 m depth). Figure 2 shows the layout

of a dipole-dipole electrode configuration and the formula used to calculate the apparent resistivity for this specific configuration (Moreira et al., 2015).

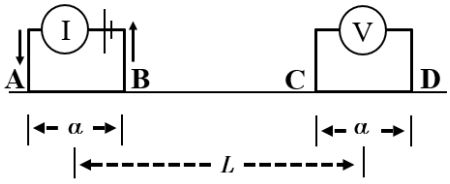

$$\rho_a = \pi \frac{V}{I} \frac{L(L^2 - a^2)}{a^2}$$

Figure 2. Diagram of a dipole-dipole configuration and the derived equation for calculating apparent resistivity (after Moreira et al., 2015). AB=current electrodes; CD=potential electrodes.

The variables shown in Figure 2 are:

ρ_a = apparent resistivity

V = voltage

I = current

L = distance between electrode pairs

a = electrode spacing

To process the measurements obtained by the ERT instrument, I used the AGI EarthImager 2D software provided by the manufacturer. The input data is the set of apparent resistivity readings from the survey area. The software calculates an apparent resistivity for a given subsurface 2-D model of Earth resistivity, and then iteratively adjusts the latter to produce a true (i.e. not apparent) resistivity section. The iterative procedure is terminated when an Earth model is found such that its calculated apparent

resistivity provides a good match to the input data. The software normally requires several iterations to find a tomogram with an acceptable error margin, typically less than 5% RMS. I have performed sensitivity analysis of the resulting tomograms to test the reliability of the inversion results. I obtained tomograms throughout different times of the year in an attempt to understand the effect of seasonal variations in precipitation on the soil moisture availability for trees. I obtained time-lapse data by conducting ERT analysis at the same locations on different days. The data were compared to precipitation and temperature data (Figure 3) from the nearby Texas Water Observatory tower and the National Centers for Environmental Information – National Oceanic and Atmospheric Administration (NCEI NOAA) to examine the relationship between Earth resistivity, rainfall, soil moisture, and water absorption rate.

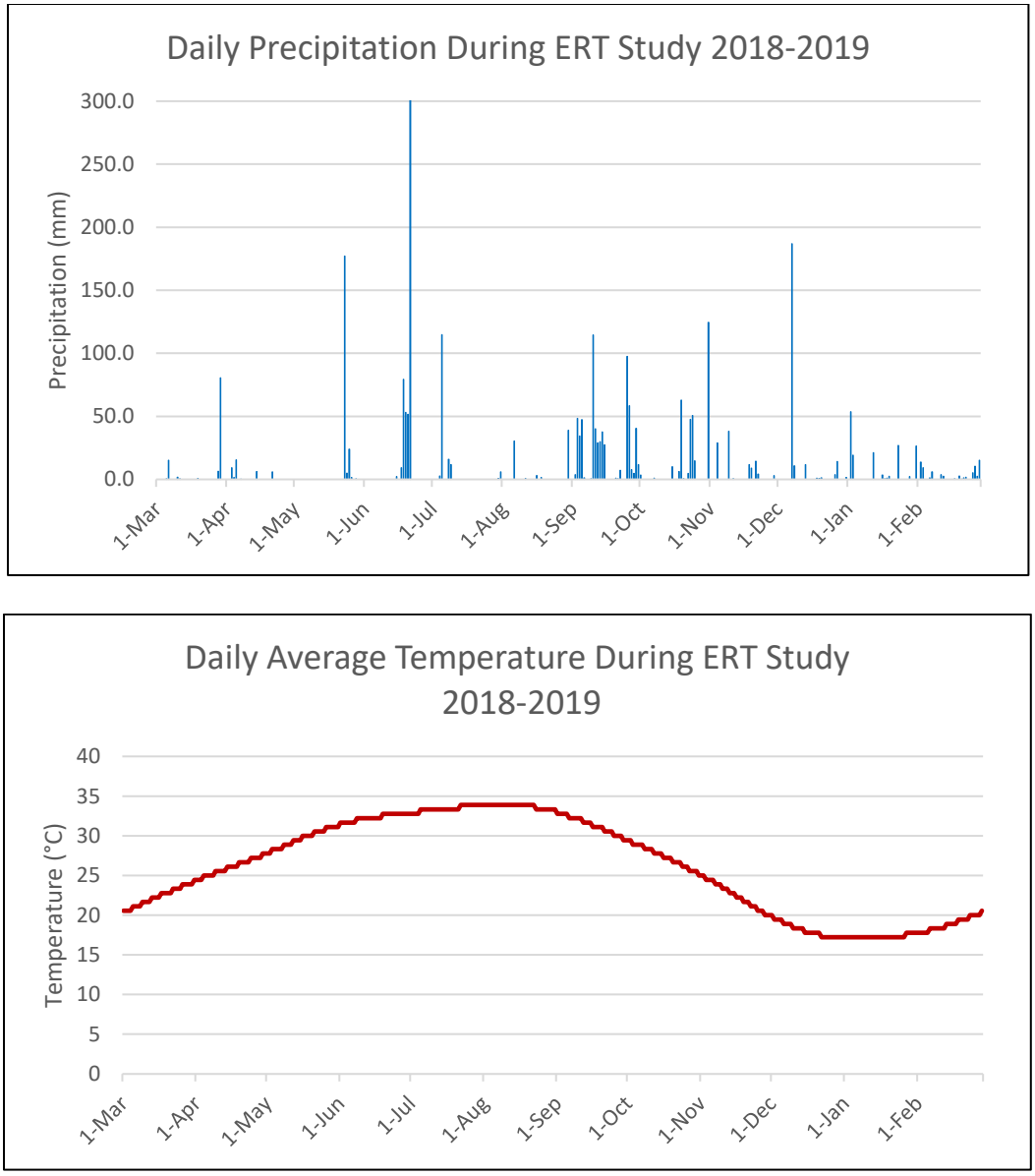

Figure 3. Top image shows the daily precipitation (in mm) and bottom image shows the daily average temperature (°C) from March 2018 to February 2019.

3. GEOLOGIC SETTING

The focus of this study is a forest site located in the San Bernard floodplain near the Brazos River at Danciger, TX. Although the watershed extends for ~180 km in length, I focus on an area in Brazoria county where three study sites are located (Figure 4). The main site is the closest of the three to the community of Danciger. As the study progressed, I incorporated the nearby Dance Bayou and Otto sites to expand understanding of the area and to compare ERT results from those other forest sites to the main Danciger site. These forests all consist of mixed hardwood trees in a humid subtropical climate per the Köppen climate classification system.

The soil is Quaternary alluvium, consisting of silt, clay, sand, and gravel. The predominant soil type is clay, such that the shallow subsurface is very conductive. Clays are more compacted than sands, so I can expect low rainfall infiltration rates, in addition to shallow root systems (Dobson, 1995). The pore spaces in clay are larger than those in sand, but the effective porosity and hence the permeability is lower. Higher compaction reduces the available pore space and infiltration capability.

The chemical and physical descriptions of the soil are available from the Natural Resources Conservation Service Soils – United States Department of Agriculture (USDA). The pH of the soil waters ranges from 5.1 to 8.4 and the amount of soluble salts (i.e. salinity), as measured by electrical conductivity, ranges from 0.1 to 0.4 S/m at 25°C. The water storage capacity that can be used by plants depends on the physical properties that determine water retention, such as soil texture, organic matter content, bulk density and soil structure. For these soils, the water storage capacity ranges from 0.11 to 0.20,

measured in mm of water per mm of soil. The saturated hydraulic conductivity ranges from 0.01-0.4 μm/s.

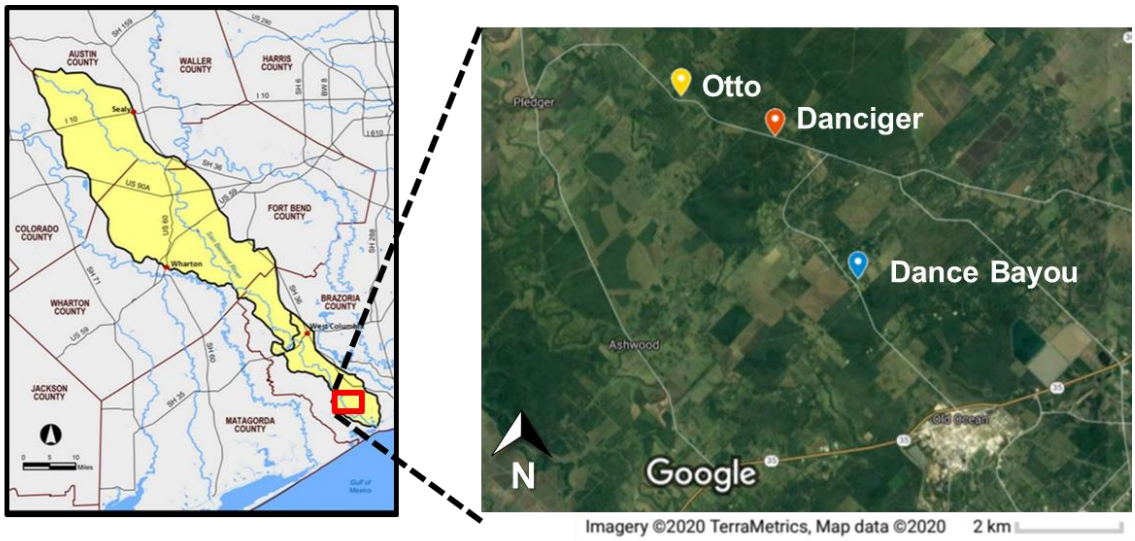

(2017) *San Bernard River Watershed Protection Plan*

Figure 4. The image on the left shows the full extent of the San Bernard Watershed through Texas. The red square delineates the larger study area (*San Bernard River Watershed Protection Plan*, 2017). The image on the right shows a zoomed-in portion of the larger study area with the three smaller study sites labeled (Google Maps, 2020).

Researchers from the Biological and Agricultural Engineering (BAEN) department at Texas A&M University conducted a soil analysis based on a soil core taken at the Danciger site. The analysis was performed using the hydrometer method. This method uses deionized water to dissolve soil samples, yielding different sets of particle textures that can be assigned to clay, loam, silt, and sand categories. The results for

different soil horizons from the surface to 1.2 m, and from 2.0 to 2.9 m depths are shown in Table 1.

Depth (cm)	**Soil Type**
0 – 30	Clay loam
30 – 60	Clay loam
60 – 90	Silty clay loam
90 – 120	Silty clay loam
200 – 230	Silty loam
230 – 260	Silty loam
260 – 290	Sandy loam

Table 1. Results from hydrometer soil analysis for different soil horizons in Danciger.

The clay content was ~40-50% throughout the soil core. The water table depth at Danciger was measured at 7.62 m on August 8 2018 and at 6.81 m on February 20 2019. Furthermore, researchers from the Ecosystem Science and Management (ESSM) department at Texas A&M University provided me with a drilling report prepared by Geotech Engineering and Testing Services. Several soil cores were extracted at different locations. The soil samples from the 50 ft. (15.2 m) boring located closest to my study site in Danciger (Figure 5, Danciger-3) are described in Table 2.

The Texas Water Observatory (TWO) operates a network of critical-zone observatories that monitor environmental variables associated with groundwater, soil water, surface water, and atmospheric water. A TWO installation is present at the Danciger

site, which provides data about the water fluxes of the area. The observatory was completed by November 2018 and useful data started being recorded in February 2019. I obtained precipitation and soil moisture information starting from that date. TWO also installed soil nodes in several areas. A node is a set of five sensors that measure soil moisture, temperature, and matric potential data at different depths: 5 cm, 15 cm, 30 cm, 75 cm, and 100 cm. Figure 5 shows several locations within the Danciger site where the different measurements were obtained by the ESSM and BAEN departments, relative to the TWO eddy covariance tower marked by a yellow star. The Danciger-3 soil node is the one closest to the tower and the ERT measurements, so I will be using the results from those instruments for the analysis.

Depth (ft. [m])	**Soil Type**	**Description**
0 – 3 (0.0 – 0.9)	Lean Clay	firm to stiff, light and dark gray, root fibers to 2 ft.
3 – 17 (0.9 – 5.2)	Fat Clay	stiff to very stiff, light and dark gray, brown
17 – 25 (5.2 – 7.6)	Sandy Lean Clay	firm to stiff, light gray, light reddish brown, with sands
25 – 43 (7.6 – 13.1)	Silty sand	light and dark gray, light brown
43 – 50 (13.1 – 15.2)	Fat Clay	stiff to very stiff, light gray, reddish brown

Table 2. Soil sample descriptions obtained from 50 ft. boring at the Danciger-3 soil node from Figure 5.

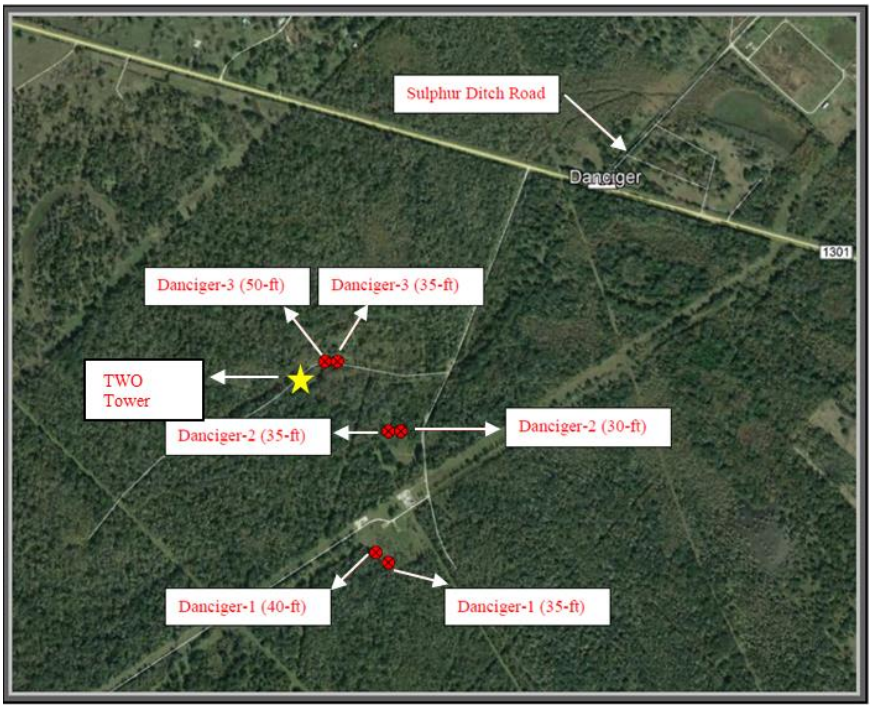

Figure 5. Google Earth Pro (2018) image of the Danciger site showing the locations of the different soil nodes operated by the ESSM and BAEN departments of Texas A&M University. The star indicates the location of the TWO tower with respect to the soil nodes.

4. RESULTS AND ANALYSIS

4.1. Preliminary Results

A first ERT measurement was performed at Danciger to determine a suitable location and electrode configuration that would address the project objectives. The ERT profile was obtained on October 15, 2017 at the location shown in Figure 6C by the red line. The electrode array was 55 m in length, with the 56 electrodes placed in the ground 1 m apart along the main trail through the forest. The resulting ERT tomogram is shown in Figure 6, processed using the EarthImager 2D software. The blue areas indicate lower resistivity (i.e. higher conductivity) and the red areas indicate higher resistivity (i.e. lower conductivity). I interpret the blue areas to have a higher water content. The water table in Danciger was measured below the depth of the ERT image at 7.62 m. This tomogram turned out not to be useful. The tomogram showed strong lateral variations instead of a layered medium as expected from a floodplain. The high-resistivity anomalies were found to be caused by buried concrete. I discovered that the site was not a pristine forest land as previously thought. The area was formerly used as a hunting camp (see Figure 6A compared to Figure 6B). A careful inspection revealed partially exposed remnants of concrete from old foundations and culverts, such that substantially large man-made structures likely lie buried under the ground across and along the trail.

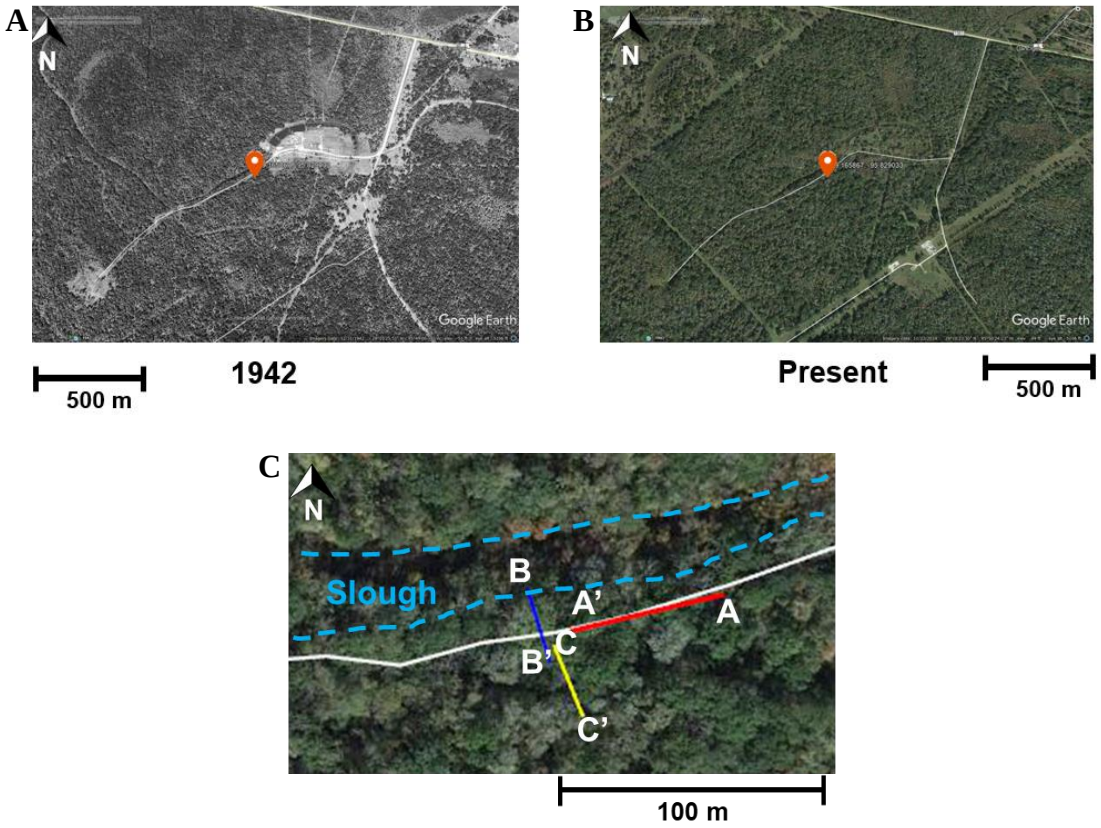

Figure 6. Google Earth Pro (2018) images of Danciger, TX with a red pin indicating the area used for the ERT measurements. (A) shows Danciger in 1942 as an old hunting camp ground. (B) shows present day Danciger. (C) shows a zoomed-in version of the survey location with colored lines representing a different survey: red for Figure 7, blue for Figure 8, and yellow for Figure 9.

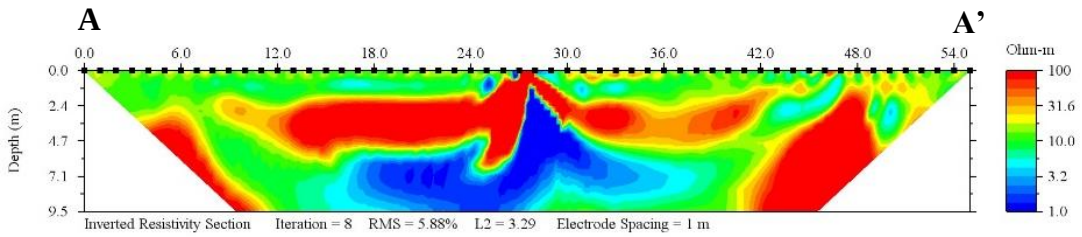

Figure 7. The high-resistivity anomalies caused by the concrete disrupt the soil moisture measurement. The scale was adjusted to represent the clay better, but the concrete had resistivity values of about 500 Ohm-meters. The survey was oriented East to West.

A second ERT profile (blue line in Figure 6C) was obtained on February 15, 2018. I established the profile across the trail along a transect in a location that showed no evidence of concrete. The electrode array length was 27.5 m with the electrodes inserted at 0.5-m spacing to provide good lateral resolution (Figure 8). Since most of the hydraulic activity of the trees is focused near the surface, I sacrificed depth for lateral resolution by reducing the electrode spacing. For this survey, a slough (freshwater pond) was present just beyond the southern end of the line. The slough contained standing water remaining after the relatively cold winter weather had brought abundant rain and reduced evaporation. Similarly to Figure 7, the tomogram shows strong lateral variations and high resistivity anomalies. Despite the presence of the slough, the resistivity is higher in the southern part of the profile. The clay may be too compacted to allow water to infiltrate into the pore spaces and thereby increase the conductivity. Another possibility is that some of the buried concrete could still be affecting the resistivity measurements. Conversely, near-surface soil moisture is apparent on the north side of the line. Overall, the area had a high conductivity; the highest resistivity measurement was only 64 Ω-m.

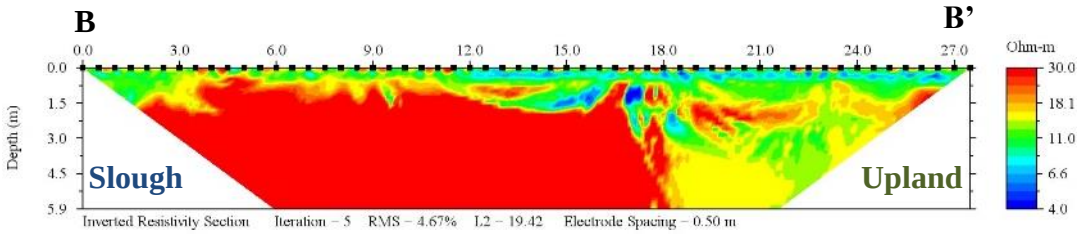

Figure 8. Resistivity section at Danciger site in February 15, 2018. Note the change in the resistivity scale compared to Figure 7. This tomogram is used to compare to the results from subsequent ERT surveys. The survey was oriented North to South.

Since my goal is to measure the resistivity in a relatively undisturbed area of the forest, I decided to avoid the trail altogether since vehicles appear to have compacted the soil which may have affected the results. Off-trail data should be more characteristic of undisturbed forest soil dynamics. The third ERT profile (C-C') is shown in Figure 6C by the yellow line, and this one was used for the rest of the Danciger study. The acquisition parameters were kept consistent with survey B regarding the electrode array length and spacing.

4.2. Danciger

Over a period of one year, I collected ERT data from the Danciger site every season, starting on March 9 2018 during the spring season and ending on February 12 2019 in late winter. The tomograms acquired are shown in Figure 9 along with the data-acquisition dates, the precipitation the area received in the 10 days prior to each ERT survey and the average daily temperature (based on TWO and NCEI data). The range of inverted bulk resistivity is ~4-30 Ω-m. The scale for all tomograms was standardized to this range to better compare the results from different surveys. To correlate the resistivity

measurement with the trees near the ERT profile, I mapped the locations and measured the diameters of trees growing within 5 m of the profile. Trees with diameters <20 cm were considered small; those with diameters 20-40 cm were considered medium; and those with diameters >40 cm were considered large. The majority of the trees were identified as water oaks and Shumard oaks, with fewer green ash trees. Table 3 shows the tree diameter and species from left to right in the ERT profile.

No.	**Diameter (cm)**	**Species**
1	48.0	Water oak
2	38.7	Water oak
3	7.5	Unidentified
4	22.9	Green ash
5	10.2	Unidentified
6	55.8	Water oak
7	6.0	Unidentified
8	67.7	Water oak
9	27.2	Water oak
10	12.0	Oak species
11	7.2	Unidentified
12	24.3	Unidentified
13	37.0	Water oak

Table 3. Tree diameters and species at Danciger site within 5 m of the ERT profile.

During March in the spring season, the trees begin to grow leaves as the weather warms up. More water is required by the trees in the spring to carry out their physiological functions. The first March tomogram in Figure 9 indicates that most of the water is concentrated near the surface where the resistivity values are low. Thus, the ERT-inferred soil moisture is high. The areas directly below the trees appear to have less soil moisture than areas where trees are absent. This finding suggests that tree water uptake depletes soil water content in the root zone during growing season. Accordingly, these areas should dry out faster after a precipitation event, especially if infiltration in the clay soil is low. Surficial moisture present beneath the trees could be redistributed by the roots, increasing the resistivity of the zones underneath those areas. The deeper areas in the tomogram reveal higher resistivity beneath the trees lending support for this process. Transpiration and root water uptake retain most of the water near the surface to be absorbed by the roots, so less water would infiltrate deeper than the root zone. I can infer from the tomograms that the pore space at depth has low water content.

I acquired another ERT profile in March 31, 2018 after a storm event of 80.5 mm that occurred in March 29, 2018. The area experienced some flooding due to the storm precipitation. However, the resulting resistivity tomogram was similar to the previous on acquired on March 9. There is no evidence of increased soil moisture near the surface. This observation implies that storm water infiltration is not very high in the clay soils. The storm water may have escaped laterally as runoff to nearby streams. Also, a fraction of the water could have been intercepted by the denser tree canopy and absorbed directly by the

leaves, or evaporated. Again, surficial moisture present beneath the trees could be redistributed by roots, increasing the resistivity of the deeper zones beneath those areas.

I was not able to obtain data during the summer season due to practical issues with the ERT equipment during the acquisition process.

The next ERT data acquisition took place on September 28 during the early fall season. A substantial amount of precipitation to the area occurred in this season, as shown by Figure 3; the precipitation 10 days prior to the ERT survey was 177.5 mm. I observed the effect of the higher precipitation regime on water infiltration, evidenced by the pervasive low-resistivity areas near the surface. Even directly under the trees, the inferred water content is much higher than it was during the spring season. During this season, the trees had not yet started shedding their leaves, so I can assume that water consumption was higher. I also observed that the areas directly below the trees have a slightly higher resistivity than the areas with no trees, which can indicate a lower water content. The high resistivity of the deeper areas did not change significantly since the March tomograms were acquired. I can assume most of the water is being redistributed by the roots or that the meteoric water does not infiltrate below ~1.5 m depths due to the clay soil.

The final ERT data acquisition was performed in February 13 during the winter at which time the trees had lost most of their leaves and the precipitation regime was drier. There is a significant increase in the resistivity near the surface, indicating a reduction in water content. However, there remains a higher water content level in those areas where no trees were present than in the areas with trees present. I also notice reduced resistivity values in the deeper areas. Since the trees had no leaves, they were not retaining as much

water near the surface. This suggests that some water infiltrated into the drier pores in the deeper areas.

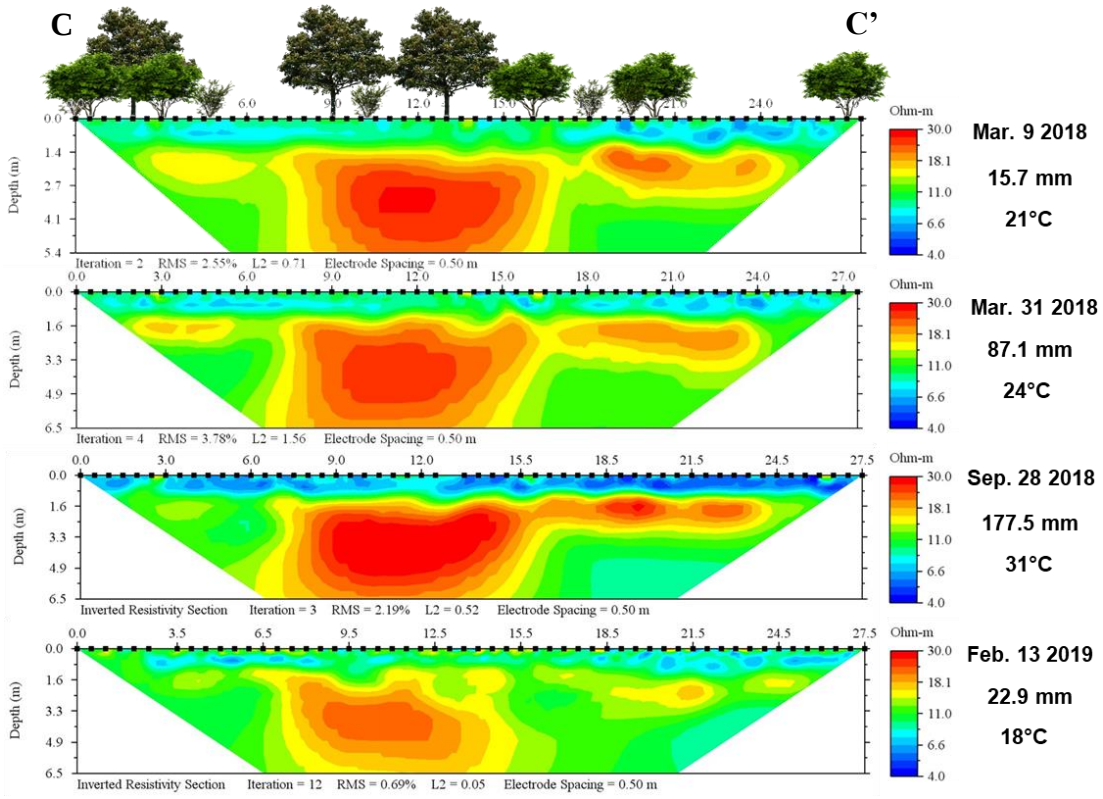

Figure 9. Time-lapse resistivity tomograms at Danciger over one year. The x-axis shows the lateral distance and the y-axis shows depth, both in meters. Each image is labeled by its acquisition date, precipitation data for the prior 10 days and the average daily temperature. Blue areas show low resistivity and are interpreted as having high water content or soil moisture. Red areas show high resistivity and are interpreted as having low water content. The tree locations for all surveys are shown in the top image (not to scale). The water table is not visible as it is deeper than the survey's depth. The surveys were oriented North to South.

4.3. Dance Bayou

The second site is at Dance Bayou, located south of Danciger as shown in Figure 4. According to the BAEN and ESSM researchers working at Dance Bayou, no vehicles are allowed into this area, except for a lawnmower that is used every 4-5 months. Figure 10 shows a Google Earth Pro (2018) image of the forest at Dance Bayou, the red line indicating the location of the ERT profile. The range of inverted resistivity values is ~5-20 Ω-m but the tomograms are plotted using the same 4-30 Ω-m scale as the Danciger tomograms. I used the same parameters as at Danciger to facilitate comparisons across the sites. The ERT results at Dance Bayou are shown in Figure 11. The locations of the mapped trees are shown in the top image similar to the presentation of the Danciger results. Most of the trees are also water oaks and Shumard oaks. Table 4 shows the measured tree diameters and their species, organized from left to right in the ERT image.

Figure 10. Google Earth Pro (2018) image of Dance Bayou. The red line shows the location of the ERT line used for all the Dance Bayou surveys.

No.	Diameter (cm)	Species
1	21.4	Unidentified
2	10.4	Unidentified
3	14.5	Oak species
4	10.7	Water oak
5	17.2	Water oak
6	63.0	Water oak
7	82.6	Water oak
8	29.7	Oak species
9	17.2	Unidentified
10	32.9	Unidentified
11	11.2	Oak species
12	20.8	Oak species
13	43.3	Oak species

Table 4. Tree diameters and species at Dance Bayou site within 5 m of the ERT profile.

In the first tomogram acquired in March 9, high resistivity pockets are found beneath lower resistivity values near the surface. This could indicate root-zone uptake or low infiltration capability of the clay soil. The near-surface resistivity is higher than it was at Danciger, suggesting lower surficial moisture. Significantly lower resistivity values are observed at ~3 m depth, indicating the presence of an aquifer below the high resistivity zones.

After the storm event in the days before March 31, the resulting tomogram shows an increase in the ERT-inferred surficial soil moisture above the high resistivity zone. This is especially the case closer to the dense trees cover to the left of the image. The meteoric water perhaps infiltrated more efficiently in this area than at Danciger. This would allow soil moisture to accumulate for the duration of the storm event. Dance Bayou is more flood-prone than Danciger, so water runoff is not as efficient. The pockets of high water content near the surface are surrounded by resistive zones. This observation could indicate root-zone uptake near the surface, as at Danciger. The surficial resistive zones also match the locations of the trees, so the roots are likely absorbing the water and thereby reducing the soil moisture. In early spring, trees are still growing out their leaves and precipitation is high, so that more water is able to accumulate than it would later in the spring or fall. No significant change between March 9 and March 31 is observed for the depth to the water table.

The third ERT data acquisition was obtained in the fall season during a period of high precipitation. I do not observe the same amount of infiltration at Dance Bayou as previously observed at Danciger during this period of time, even though Dance Bayou tends to flood easily. The trees were covered in leaves so most of the water was likely absorbed by the roots or trapped by the canopy and was either absorbed or evaporated from the leaves.

Just as at Danciger, I was unable to acquire summer-season data due to equipment malfunction. I also could not obtain winter data at Dance Bayou due to time constraints and equipment availability.

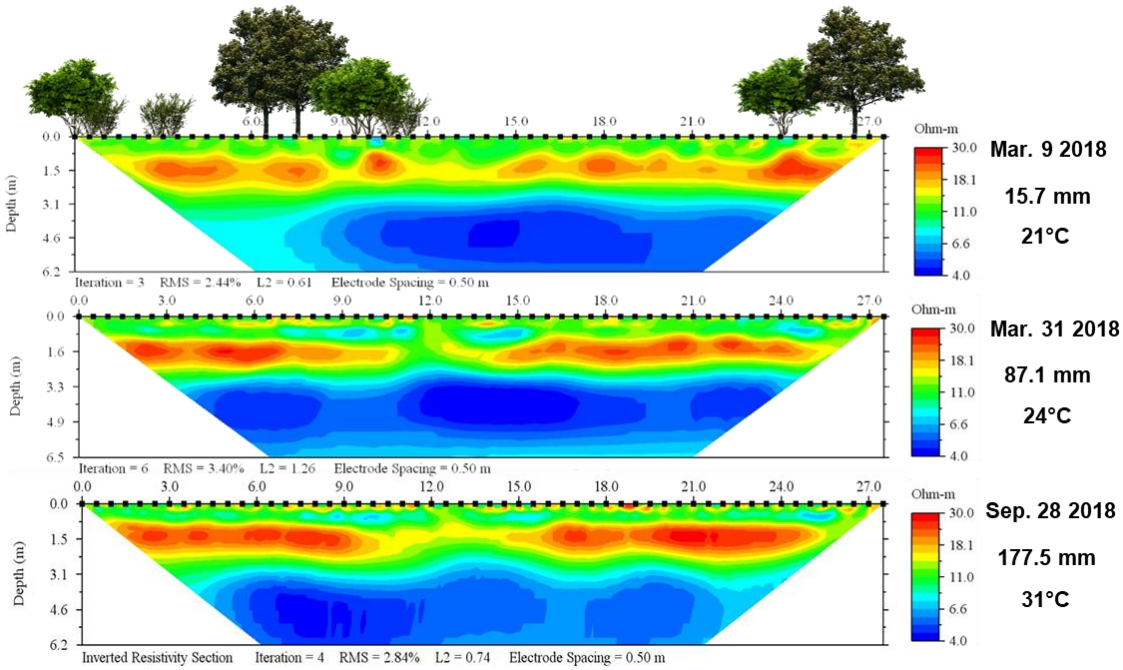

Figure 11. As per Figure 9 except time-lapse resistivity tomograms of Dance Bayou over 7 months. The surveys were oriented North to South.

4.4. Otto

The third ERT data acquisition site was at Otto, located west of Danciger as shown in Figure 4. This site was incorporated into my study later than the other two sites so the amount of data is limited. Figure 12 shows a Google Earth Pro (2018) image of the Otto site, with the yellow line indicating the ERT profile extending from west to east. This land was private and fenced, so the geophysical equipment could not be brought very far from the access road into the forested area. The range of inverted resistivity measurements is ~3-30 Ω-m. The same acquisition parameters were used for the ERT measurements as

per the previous sites, and again the trees within 5 m of the ERT profile were mapped (tree information on Table 5). The two ERT results are shown in Figure 13.

Figure 12. Google Earth Pro (2018) image of Otto. The yellow line shows the location of the ERT line used for all the Otto surveys.

No.	Diameter (cm)	Species
1	20.7	Unidentified
2	10.1	Oak species
3	39.8	Oak species
4	31.4	Oak species
5	28.1	Oak species
6	18.9	Unidentified
7	24.0	Oak species
8	24.6	Oak species
9	22.1	Oak species
10	25.9	Oak species

Table 5. Tree diameters and species at Otto site within 5 m of the ERT profile.

The first ERT survey at Otto was performed in September 28 during the fall season with high precipitation and full tree canopies. I do not observe particularly high ERT-inferred surficial soil moisture. However, I do observe several high-resistivity pockets, probably produced by the roots redistributing soil moisture towards the surface. Water infiltration seems to be low in this area. Low resistivity values at about ~2 m depth could be indicative of an aquifer. The first tomogram shows a slight increase in the resistivity values below the suggested aquifer, possibly indicating it is a perched aquifer.

The second ERT profile was acquired on February 13 during the winter when rainfall was low, with leaves mostly absent and consequently water consumption was low.

I can observe higher-resistivity zones very close to the surface as the trees absorb the little soil moisture available to them after a prolonged dry period. The resistivity pockets from the first image are mostly absent. Perhaps during earlier rainfall, the water infiltrated deeper into the soil and allowed the water table to rise. The hypothesized aquifer also seems to contain more water than it did during the fall. Since the earlier image was obtained after a dry summer season, the aquifer was possibly depleted at that time, and water started accumulating again once the rainier season started. By the time of acquisition of the second image, the aquifer may have been at its full capacity.

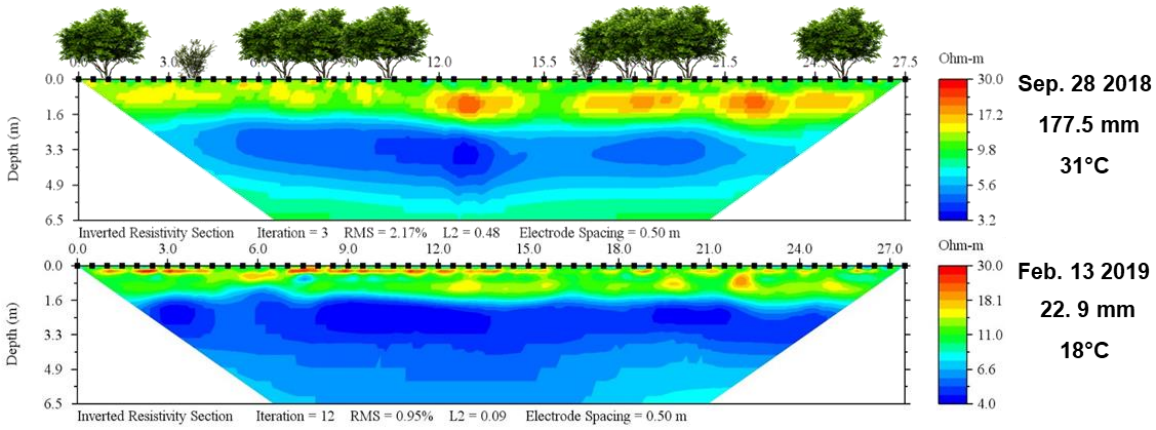

Figure 13. As per Figure 9 except time-lapse resistivity tomograms at Otto over 6 months. The surveys were oriented West to East.

4.5. Soil Moisture

I exported the point-wise resistivity-model information from the ERT tomograms in order to calculate soil moisture as water saturation in the Waxman-Smits equation. It should be mentioned that interpretation of point-wise model information extracted from a

non-unique, smoothed geophysical inversion result must be done with caution. The point-wise resistivity information was loaded into a Python code I developed and then it was converted to conductivity and soil moisture using equation (4). The resulting images were intended to reveal an image of the water content in the pore spaces after the effects of clay conduction are removed. However, in order to yield accurate results, it was required to know the parameters that appear in equation 4. Unfortunately, the parameters a, m, and $\tilde{\sigma}$ require lab measurements for their empirical determination, as they vary widely depending on the type of soil under study (Mualem and Friedman, 1991; Laloy et al., 2011; Doussan and Ruy, 2009; Onovughe and Sofolabo, 2016). Such an analysis proved beyond the scope of my study, so a soil moisture determination was instead derived from empirical relationships found in the literature.

Laloy et al. (2011) performed controlled laboratory experiments to correlate the water content and electrical resistivity of soils with different bulk densities. In my field ERT study, the highest resistivity value was ~30 Ω-m (~0.03 S/m) and the lowest was ~3.5 Ω-m (~0.30 S/m). Based on charts shown in Laloy et al., I should expect the water content of the field soils to be ~25-45%. Mualem and Friedman (1991) proposed a conceptual model to predict bulk electrical conductivity of saturated and unsaturated soils. Comparing my resistivity results to their laboratory experiments on silty loam and sandy loam soils (Figure 14), the expected water content of the field soils is ~15-35%.

I obtained soil moisture measurements from TWO project researchers. The data were acquired using the soil moisture probes located at Danciger-3 shown in Figure 5. Unfortunately, data collection started December 21 2018. Thus, I have data only for the

winter survey at Danciger. Furthermore, the moisture-probe measurements extend only to 100 cm depth so that only near-surface water content data are available. The soil node sensors measured data every 30 minutes every day for 24 hours. I calculated the average water content of the five soil horizons for February 13 2019 using the water content measurements for the entire day. The average measurements are shown in Table 6.

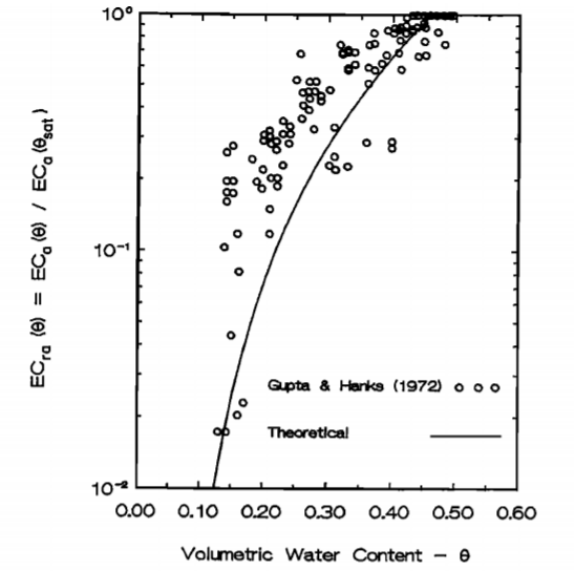

Figure 14. The experimental data of relative electrical conductivity as a function of soil water content for sandy loam and silty loam. The curve shows a theoretical relationship between unsaturated soil and water content. Reprinted with permission from 'Theoretical prediction of electrical conductivity in saturated and unsaturated soil' by Y. Mualem and S. P. Friedman, 1991. *Water Resources Research,* 27, p. 2771-2777, Copyright 1991 by John Wiley and Sons.

Depth (cm)	Water Content (%)
5	44
15	32
30	55
75	59
100	57

Table 6. Average water content measurements from soil-moisture probes obtained at the Danciger-3 soil node on February 13 2019.

Based on the ERT tomogram acquired during the winter at Danciger, the resistivity measurements within 1 m of the surface lie between ~5-11 Ω-m. These values correspond to water content ~20-25% for the silty loams, such as those analyzed by Laloy et al. and Mualem-Friedman. The TWO measurements are significantly higher than the predicted values from the Laloy et al. and Mualem-Friedman studies, yet they cover a much smaller area than the ERT measurements. Thus, the results from the soil nodes should not be strictly compared to the ERT estimates. A more sophisticated and complex approach than the one described here is recommended to correlate electrical resistivity measurements to soil moisture content. Nevertheless, my results have been shown to be useful to analyze water dynamics throughout the year. ERT tomograms provide an average value over a broader area with a mixture of wet and dry soil, so this method yields a good estimate of the water content and relative spatial variations averaged over a wider area. The ERT data can be used in sap flow and tree physiology studies that require a knowledge of subsurface moisture temporal changes.

5. CONCLUSIONS

ERT is a non-invasive geophysical survey method that is useful for examining and correlating bulk resistivity variations to soil moisture-content across spatiotemporal scales. Time-lapse ERT provides insight on ecohydrological processes relating to seasonal weather changes. Pore fluid conducts electric current, so low-resistivity (i.e. high conductivity) areas may be interpreted as having high water content. All three sites occupied in this study consist of primarily clay soils, which would indicate low water permeability and low infiltration rates, as well as higher bulk-conductivity measurements due to the surface conduction at the surface of clay particles. The clay surface charge accounted for lower resistivity results than would have been observed in sandy soils.

I observed in the ERT images that rainfall events did not have a large impact on the ERT-inferred soil moisture throughout the study period. This was likely due to the low permeability and infiltration characteristic of clays. Danciger is more transited by vehicles than Dance Bayou, which could lead to greater soil compaction and lower infiltration rates. The ERT images support this conjecture. In Dance Bayou, there were low-resistivity pockets after the rainfall event that occurred in March, suggesting some water infiltration. Danciger did not show any evidence of water infiltration after the same rainfall event. The most significant change occurred after the winter season, when root water uptake is reduced. The lower water demand from the trees could have allowed water to infiltrate deeper than it did during the growing season.

The results from the ERT images suggest that tree physiological functions and structure influence water fluxes and groundwater recharge. I observed high-resistivity

zones surrounding low-resistivity zones located near the surface, interpreted as root water uptake redistributing moisture closer to the surface. During periods of low rainfall, surficial resistive zones, interpreted as drier soils, were found closer to trees. The roots likely absorb surrounding water and reduce soil moisture. Since root water uptake occurs due to the difference in water potential between the leaves and the soil, trees are more likely to absorb more water during the growing season when they have more leaves on their branches. During the winter, most of the leaves fall off in preparation for drier weather. Therefore, less water is absorbed by the roots and some infiltration can occur, as shown by reduced resistivity values in the deeper areas. Once the leaves start growing back, the tree canopy can intercept meteoric water and reduce the amount of water reaching the soil. Moreover, the evapotranspiration taking place at the leaves promotes root water uptake, depleting soil moisture. I suggest performing additional ERT transects that run parallel and perpendicular to the trees to approximate a 3-dimensional view of the root zone and its relationship with the inferred soil moisture profiles.

Weather patterns and climate change can alter plant activities, thus influencing soil water dynamics in an area. It is important to understand the effects plants have on soil moisture variations within the root zone as these ecohydrological interactions have the potential to alter landscape dynamics. Even though accurate soil moisture calculations would require a deeper analysis, ERT provides useful spatiotemporal information on water content changes and fluxes over a broad area that helps ecohydrologists better understand the effect that climate change and land usage can have on hydrologic fluxes and ecosystem sustainability.

REFERENCES

(2017) *San Bernard River Watershed Protection Plan.* [pdf] Houston-Galveston Area Council. Available at: https://www.tceq.texas.gov/assets/public/waterquality/nps/watersheds/San%20Bernard%20WPPfinal.pdf [Accessed 8 April 2019]

A Dictionary of Earth Sciences (1999) Encyclopedia.com, Oxford University Press. Available at: http://www.encyclopedia.com/science/dictionaries-thesauruses-pictures-and-press-releases/geometric-factor [Accessed 20 February 2018]

AGIUSA. (2017). 'Dipole-Dipole Array: Electrical Resistivity Methods, Part 3.' [online] Available at: https://www.agiusa.com/dipole-dipole%E2%80%8B-%E2%80%8Barray%E2%80%8B [Accessed 9 September 2019]

Amidu, S. A., and Dunbar, J. A. (2007) 'Geoelectric studies of seasonal wetting and drying of a Texas vertisol.' *Vadose Zone Journal*, 6 (3), p. 511-523. https://doi.org/10.2136/vzj2007.0005

Bass, B., Cardenas, M. B., and Befus, K. M. (2017) 'Seasonal Shifts in Soil Moisture throughout a Semiarid Hillslope Ecotone during Drought: A Geoelectrical View.' *Vadose Zone Journal*, 16. doi:10.2136/vzj2016.11.0108

Cardenas, M. B., and Kanarek, M. R. (2014) 'Soil moisture variation and dynamics across a wildfire burn boundary in loblolly pine (Pinues taeda) forest.' *Journal of Hydrology*, 519, p. 490-502. http://dx.doi.org/10.1016/j.jhydrol.2014.07.016

Chapin III, S. F., Matson, P. A., and Mooney, H. A. (2002) 'Principles of Terrestrial Ecosystem Ecology.' *New York, Springer*. ISBN: 0-387-95439-2

Cregg, B. and Zhang, J. (2000) 'Carbon Isotope Discrimination as a Tool to Screen for Improved Drought Tolerance.' *Department of Horticulture, Michigan State University*. Retrieved March 3, 2018 from https://henderson.ces.ncsu.edu/fletcher/programs/nursery/metria/metria11/cregg/

Crow, P. (2005) 'The influence of soils and species on tree root depth.' *Forestry Commission*, ISBN: 0-85538-679-7

Dobson, M. (1995) 'Tree Root Systems.' *Arboriculture Research and Information Note* 130/95/ARB

Doussan, C., and S. Ruy (2009). 'Prediction of unsaturated soil hydraulic conductivity with electrical conductivity.' *Water Resour. Res.*, 45, W10408, doi:10.1029/2008WR007309.

Everett, Mark. (2013) 'Near-surface Applied Geophysics.' *Cambridge University Press*, doi: 10.1017/CBO9781139088435. ISBN: 978-1-107-01877-8

Everett, M. E., Pierce, C. J., and 'Save, N., et al. (2006). 'Geophysical investigation of the June 6, 1944 D-Day invasion site at Pointe du Hoc, Normandy, France.' *Near Surface Geophysics*, 4, p. 289–304.

Fan, Y., Miguez-Macho, G., Jobbágy, E. G., Jackson, R. B., and Otero-Casal, C. (2017) 'Hydrologic regulation of plant rooting depth.' *PNAS*, 114 (40) p. 10572-10577. https://doi.org/10.1073/pnas.1712381114

Fetter, C. W. (2001) 'Applied Hydrogeology' 4th ed. Upper Saddle River, N. J.: Prentice Hall. 1942-2001. ISBN-13: 978-0130882394

Google LLC (2019) Google Earth Pro V 7.3.2.5776. NVIDIA Corporation

Google Maps (2020) *Research Sites.* 1:1066667. Google Maps [online] Available through https://www.google.com/maps [Accessed 8 January 2020]

Jackson, R.B., Sperry, J.S., and Dawson, T.E. (2000) 'Root water uptake and transport: using physiological processes in global predictions.' *Trends in Plant Science*, 5 (11), p. 482-488, doi: 10.1016/s1360-1385(00)01766-0

Jayawickreme, D. H., Van Dam, R. L., and Hyndmand, D. W. (2008) 'Subsurface imaging of vegetation, climate, and root-zone moisture interactions.' *Geophysical Research Letters*, 35, L18404, doi: 10.1029/2008GL034690

Jipp, P. H., Nepstad, D. C., Cassel, D. K., and Reis de Carvalho, C. (1998) 'Deep soil moisture storage and transpiration in forests and pastures of seasonally-dry Amazonia.' *Climatic Change*, 39, p. 395-412, doi: 10.1023/A:1005308930871

LaBreque, D.J. and X. Yang (2001). 'Difference inversion of ERT data: A fast inversion method for 3-D in situ monitoring.' *J. Environmental Engineering Geophysics*, 6, p. 83-89.

Laloy, E., Javaux, M., Vanclooster, M., Roisin, C., and Bielders, C.L. (2011) 'Electrical Resistivity in a Loamy Soil: Identification of the Appropriate Pedo-Electrical Model.' *Vadose Zone Journal*, 10, p. 1023-2033, doi: 10.2136/vzj2010.0095

Moreira, C. A., Montenegro Lapola, M., and Carrara, A. (2016). 'Comparative analyzes among electrical resistivity tomography arrays in the characterization of flow structure in free aquifer.' *Geofísica internacional*, 55(2), p. 119-129.

Mualem, Y., and Friedman, S. P. (1991) 'Theoretical prediction of electrical conductivity in saturated and unsaturated soil,' *Water Resour. Res.*, 27, p. 2771-2777, doi :10.1029/91WR01095.

National Centers for Environmental Information (NCEI) – National Oceanic and Atmospheric Asministration (NOAA) Climate Data Online. https://www.ncdc.noaa.gov/cdo-web/

Natural Resources Conservation Service Soils - United States Department of Agriculture. *Published Soil Surveys for Texas*. [online] Available at: https://www.nrcs.usda.gov/wps/portal/nrcs/surveylist/soils/survey/state/?stateId=TX [Accessed 30 Mar. 2018].

Onovughe, E. and Sofolabo, A. (2016) 'Saturation Modelling: Using the Waxman-Smits Model/Equation In Saturation Determination in Dispersed Shaly Sands.' *Journal*

of Multidisciplinary Engineering Science and Technology (JMEST), 3(6). ISSN 2458-9403. http://www.jmest.org/wp-content/uploads/JMESTN42351620.pdf

Parent, C., Capelli, N., Berger, A., Michele, C., and Dat. J. F. (2008) 'An Overview of Plant Responses to Soil Waterlogging.' *Plant Stress* 2 (1), p. 20-27.

Rodríguez-Iturbe, I., D'Odorico, P., Laio, F., Ridolfi, L., and Tamea, S. (2007) 'Challenges in humid land ecohydrology: Interactions of water table and unsaturated zone with climate, soil, and vegetation.' *Water Resour. Res*., 43, W09301, doi:10.1029/ 2007WR006073

Rodríguez-Robles, U. Arredondo, T., Huber-Sannwald, E., Ramos-Leal, J.A., and Yépez, E.A. (2017). 'Application of geophysical tools for tree root studies in forest ecosystems in complex soils.' *Biogeosciences*, 14, p. 5343–5357. https://doi.org/10.5194/bg-14-5343-2017

Rothfuss, Y., and Javaux, M. (2017) 'Reviews and Syntheses: Isotopic approaches to quantify root water uptake: a review and comparison of methods.' *Biogeosciences*, 14, 2199-2224, doi:10.5194/bg-14 p. 2199-2017

Shang, K. (2016) 'The simulation of water uptake by vegetation and its impact on slope stability using an image-based model of plant root architecture.' Doctor of Philosophy Thesis, Cardiff University.

Stratópoulos, L. M. F., Zhang, C., Häberle, K., Pauleit, S., Duthweiler, S., Pretzsch, H, and Rötzer, T. (2019) 'Effects of Drought on the Phenology, Growth, and Morphological Development of Three Urban Tree Species and Cultivars.' *Sustainability (2071-1050)*, 11(18), p. 5117, doi: 10.3390/su11185117

Swaid, F. (2009). 'Estimating a new approach for describing electrical conductivity parameters in partially saturated sediments.' *WIT Transactions on Ecology and the Environment*. 127. 363-375. doi:10.2495/RAV090321

'Transport of Water and Solutes in Plants', Boundless Biology. (2017). *Courses.lumenlearning.com*. Retrieved February 21, 2018 from

https://courses.lumenlearning.com/boundless-biology/chapter/transport-of-water-and-solutes-in-plants/

Vasellati, V., Oesterheld, M., Medan, D., and Loreti, J. (2001) 'Effects of Flooding and Drought on the Anatomy of Paspalum dilatatum.' *Annals of Botany.* 88, 355-360, doi:10.1006/anbo.2001.1469

Waxman, M.H. and Smits, L.J.M. (1968) 'Electrical Conductivities in Oil-Bearing Shaly Sands.' *Society of Petroleum Engineers Journal*, 8, 107-122. http://dx.doi.org/10.2118/1863-A.